



## PAPER

Cite this: *Anal. Methods*, 2024, 16, 3231

# Monolithic stationary phases prepared *via* cyclic anhydride ring-opening polymerization as tunable platforms for chromatographic applications†

Ahmad Aqel, \* Ayman A. Ghfar, Ahmed-Yacine Badjah-Hadj-Ahmed and Zeid A. ALothman 

Polymer monolithic stationary phases were prepared based on a cyclic anhydride as a reactive and tunable platform *via* ring-opening post-polymerization using primary amines, octadecylamine and benzylamine. The characterization techniques indicated the insertion of the functional groups into the original monoliths and confirmed the amidation reactions. The post-polymerization modification also improved the monolith's thermal and mechanical stability and induced significant improvement in their surface area. The stationary phases were synthesized inside small dimension stainless-steel columns (2.1 mm i.d. × 50 mm length). The prepared columns before and after modifications have been tested for the separation of the alkylbenzene series and some polycyclic aromatic hydrocarbons (PAHs) as model compounds. In all cases, the chromatographic performance in terms of the height equivalent to a theoretical plate on the functionalized monoliths was remarkably improved when compared with that on the unmodified monolith, which was between 9.59–39.49  $\mu\text{m}$  and 4.08–31.50  $\mu\text{m}$  using monoliths modified with octadecylamine and benzylamine, respectively. Under the same chromatographic conditions, the functionalization of monoliths with octadecylamine provided more hydrophobic interactions and enhanced the retention of alkylbenzenes, while the modification of monoliths with benzyl groups improved the separation and the retention of the PAHs through the strong  $\pi$ - $\pi$  interactions. However, post-modification polymerization with octadecylamine and benzylamine enhanced the separation efficiency of the prepared columns toward all studied compounds. The repeatability of the injections on the same column and the reproducibility of the prepared columns have been studied for some selected parameters and estimated in terms of percent relative standard deviation (%RSD) for some of the studied compounds. The repeatability of the prepared columns was  $\leq 9.42\%$  ( $n = 5$ ) based on run-to-run injections and  $\leq 9.48\%$  based on day-to-day injections for five successive days. The reproducibility levels, on the other hand, were  $\leq 20.95\%$  for all studied parameters in all cases. To assess their performance for the analysis of real samples, the applicability of the prepared columns was examined for the separation of the active ingredients extracted from some commercial pharmaceutical formulations and for the separation of tea water extract constituents. The validation data show the suitability of the columns for practical use in the routine analysis of these samples.

Received 12th February 2024  
Accepted 22nd April 2024

DOI: 10.1039/d4ay00251b

[rsc.li/methods](https://rsc.li/methods)

## 1. Introduction

For the last two decades, polymer-based monoliths such as polymethacrylates, polystyrenes, and polyacrylamides, received significant attention as adsorbents and stationary phases for many applications, especially for large molecules.<sup>1–4</sup> The used polymerization mixture has a strong effect on the monolith morphology and properties; hence, several researchers tried to optimize monomers, crosslinkers, and porogenic solvent

compositions along with the polymerization conditions including temperature and time.<sup>1,4–8</sup>

The naked polymer monoliths are interconnected non-porous microglobules. The porous structure of the monolith channels mainly consists of large pores and in most cases, absence of mesopores.<sup>1,4,9–13</sup> Fewer mesopores mean low surface area and lack of interaction sites, thus making the unmodified polymer monoliths unable to interact with small molecules. However, some groups developed several scenarios to overcome the limitations of the naked monoliths and enhance their retention properties. Some researchers optimized the polymerization conditions and the monomeric mixtures,<sup>4–8</sup> used single or multi-crosslinker monomers,<sup>14–16</sup> introduced additional hyper-crosslinking reactions,<sup>17,18</sup> employed further post-polymerization modifications,<sup>19–22</sup>

Department of Chemistry, College of Science, King Saud University, P.O. Box 2455, Riyadh, 11451, Saudi Arabia. E-mail: [ajfseisi@ksu.edu.sa](mailto:ajfseisi@ksu.edu.sa)

† Electronic supplementary information (ESI) available. See DOI: <https://doi.org/10.1039/d4ay00251b>

and incorporated or immobilized a certain amount of micro- or nanoparticles into the porous channels of the monoliths such as polymeric latex nanoparticles,<sup>23,24</sup> carbonaceous nanomaterials,<sup>25–28</sup> clay minerals,<sup>29,30</sup> metallic nanoparticles,<sup>31–33</sup> silica nanoparticles,<sup>34,35</sup> and metal–organic frameworks.<sup>36–38</sup>

As a summary of nearly 25 years of research, polymer-based monoliths have witnessed various developments in many application fields and can be still improved since materials and polymer chemistry are extremely rich in options and chemical reactions. This work presents the preparation of a poly(itaconic anhydride-co-ethylene dimethacrylate) monolith as a novel tunable stationary phase platform for liquid chromatography applications. Itaconic anhydride is an unsaturated and reactive cyclic anhydride of itaconic acid, and thus, itaconic anhydride enables radical copolymerization with electron-donating monomers such as methacrylates on one hand and allows post-polymerization modification *via* amidation with suitable amines on the other hand.<sup>39–42</sup>

The modification of the monolith surface after polymerization aims to reduce the large through pores between the aggregated microglobules of the monolith channels, increase the specific surface area, add more interactive sites into the monolith structure, and introduce new and selective functionalities on the monolith structure to meet the requirements for the desired applications and enhance the chromatographic performance of the monolithic columns.

## 2. Experimental

### 2.1 Chemicals and real samples

Ethylbenzene, naphthalene, acenaphthylene, phenanthrene, benzo(*a*)anthracene, chrysene, and benzo(*k*)fluoranthene were purchased from BDH (Lutterworth, UK). Itaconic anhydride and benzylamine were obtained from Merck (Darmstadt, Germany). Ethylene dimethacrylate, azo-bis-isobutyronitrile, 1,4-butanediol, 1-propanol, octadecylamine, toluene, *n*-propylbenzene, *n*-butylbenzene, *n*-pentylbenzene, fluorine anthracene, and pyrene were provided by Aldrich (Steinheim, Germany). Ultrapure water was obtained using a Milli-Q Advantage Elix system (Millipore S.A.S. 67120 Molsheim, France). HPLC-grade acetonitrile and methanol were acquired from Fisher Scientific (Leicestershire, UK). All chemicals used for the synthesis of monoliths and chromatographic applications are used without purification.

As a real sample, Profinal-XP tablets labeled 65 mg caffeine and 400 mg ibuprofen (Julphar, Gulf Pharmaceutical Industries, Ras Al Khaimah, UAE), Relaxon capsules labeled 300 mg paracetamol and 250 mg chlorzoxazone (Jamjoom Pharmaceuticals co, Jeddah, Saudi Arabia), and Aspirin-C tablets labeled 400 mg aspirin and 240 mg vitamin-C (Bayer Pharmaceutical Company, Aktiengesellschaft AG, Germany) were collected from a local market in Riyadh, Saudi Arabia. 0.2 g of each commercial drug was weighed, transferred to a 100 mL volumetric flask partially filled with acetonitrile/water (50/50, v/v), and sonicated for 5 min. The solutions were cooled to room temperature and the volume was made up to the mark with the same solvent. A black tea sample was obtained as a powder from a local supermarket (Riyadh, Saudi Arabia). 0.1 g of the tea powder was placed in 100 mL of hot water (about 80 °C) and stirred for

1.0 min. Then, the solution was filtered with a 0.45 µm nylon membrane before it was injected.

### 2.2 Separation column preparation

Compared to the traditional particulate stationary phases, monoliths are directly synthesized inside the columns and avoid the packing step. In this work, the monomeric mixtures were composed of itaconic anhydride 3 wt%, ethylene dimethacrylate 24 wt%, 1,4-butanediol 40 wt%, 1-propanol 32 wt%, and azo-bis-isobutyronitrile 1 wt%.

Empty stainless-steel columns (dimensions: 2.1 mm i.d. × 50 mm length) were purchased from Restek (Bellefonte, PA, USA). The empty column was washed with acetone and then dried. The normal filling of the monomeric materials usually results in voids, bubbles, or contraction. To make sure that the columns will be fully filled with the stationary phases, filling of the monomeric materials in this work was assisted by connecting the empty stainless-steel columns with extra 10 cm capillary columns, 250 µm i.d. from the inlet and 100 µm i.d. from the outlet, at both ends. The monomeric mixtures were mixed, homogenized by using a vortex mixer for 5 min, purged by using a stream of highly pure N<sub>2</sub> for 5 min, and sonicated in an ultrasonic bath set at 40 °C for 10 min. The stainless-steel columns were filled with the mixture, and both capillary ends were closed with pieces of rubber, and placed in an oven maintained at 70 °C for 12 h. After preparation, the separation columns were washed with acetonitrile at a flow rate of about 0.01 mL min<sup>-1</sup> for 2 h to remove the unreacted materials.

To functionalize the itaconic anhydride reactive groups, a 10% solution of octadecylamine (or benzylamine) in acetonitrile was passed through the prepared columns at a flow rate of 0.01 mL min<sup>-1</sup> for 4 h, and allowed to stand for 1 h at 60 °C. Finally, the columns were washed with acetonitrile at a 0.01 mL min<sup>-1</sup> flow rate for another 3 h. For comparison, a control column was prepared by the same procedure but without post-polymerization modification. Fig. 1 shows the synthesis procedure of the stationary phases and post-polymerization modifications afforded in this work.

### 2.3 Column and stationary phase characterization

The morphology of the stationary phases was investigated on a Jeol JSM-6380LA analytical scanning electron microscope (SEM) at 5 kV (Tokyo, Japan). Thermal stability of the monolithic stationary phases was measured using thermogravimetric analysis (TGA) with a Mettler-Toledo TGA/DSC Stare system (Schwerzenbach, Switzerland). For this purpose, 20 mg of the control and modified monoliths were heated from 25 to 500 °C at a rate of 10 °C min<sup>-1</sup>. The Fourier-transform infrared (FT-IR) spectra of the stationary phases were recorded on a Thermo Nicolet 6700 spectrophotometer (Madison, WI, USA). The adsorption–desorption isotherm of liquid N<sub>2</sub> was also used for measurement of the surface areas of the monoliths before and after modifications using a Gemini VII 2390 Micromeritics surface area analyzer (Norcross, GA, USA) at –196 °C.

The hydrodynamic properties of the prepared columns including porosity and permeability were estimated. The flow

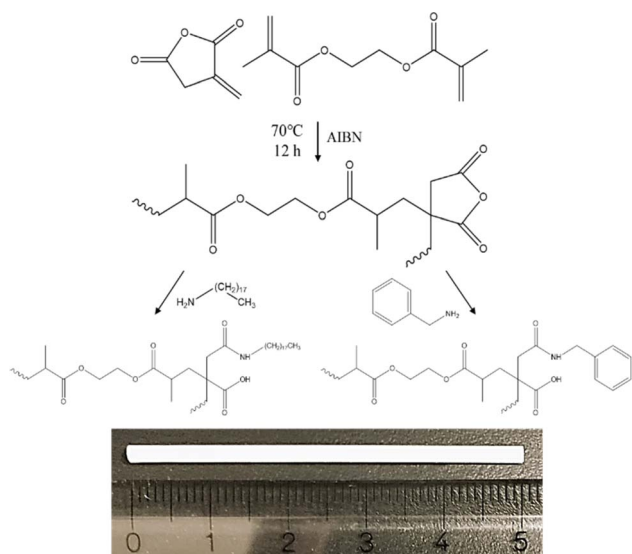


Fig. 1 Schematic representation of the functional polymer monolith synthesis and a photograph of the prepared stationary phase pushed out of the column.

method was used to determine the total porosity of the prepared columns. In this study porosity values were measured by injecting a small plug of acetonitrile as unretained material.<sup>1,4</sup> On the other hand, the permeability of the prepared columns was measured based on Darcy's equation by passing acetonitrile and water through the columns at 0.25 mL min<sup>-1</sup> flow rate and 30 °C column temperature.<sup>1,4</sup>

#### 2.4 Chromatographic conditions and validation

All chromatographic analyses were performed on a Shimadzu HPLC system consisting of an LC-20AD liquid chromatograph, a SIL-20A autosampler, a DGU-20 A5R degasser, a CTO-20A column oven, and an SPD-M20A diode-array detector (Kyoto, Japan). The Shimadzu LCsolution software was employed to control the system and acquire the data. Different ratios of acetonitrile/water in isocratic mobile phase mode at different flow rates and detector wavelengths were used for the analysis of solutes. In all the cases, the injection volume was fixed at 1.0 μL.

Various parameters were investigated to evaluate the performance of the prepared columns. For this purpose, the main chromatographic parameters including the retention time

( $t_R$ ), width at half peak ( $w_{0.5}$ ), number of theoretical plates ( $N$ ), the height equivalent to theoretical plates ( $H$ ), retention factor ( $k$ ), selectivity factor ( $\alpha$ ), chromatographic resolution ( $R_s$ ), and asymmetry factor ( $A_s$ ) were measured. The void times ( $t_0$ ) of the columns were measured by injecting a small plug of acetonitrile and recording the repeatable perturbation signals.

## 3. Results and discussion

### 3.1 Column preparation

This work aims to design and synthesize novel polymer monolithic materials as stationary phases for HPLC separation and analysis of a wide range of chemicals. For this purpose, itaconic anhydride has been selected as a reactive monomer and tunable platform, in which the epoxy ring could be modified after the polymerization reactions. Based on our previous studies and preliminary experiments, the monomeric mixture percentages and the polymerization temperature and time have been carefully optimized.<sup>4,22,26</sup>

After preparation, the itaconic anhydride reactive groups were functionalized through an amidation reaction between amine monomers and epoxy groups. In this study, amidation reactions were performed between octadecylamine or benzylamine and itaconic anhydride moieties to produce monolith structures with C<sub>18</sub> or benzene ring functionalities, respectively, as shown in Fig. 1. Both functionalities are strong candidates for interacting with a wide range of chemical compounds in a reversed-phase HPLC mode, in particular, through hydrophobic and  $\pi$ - $\pi$  retention mechanisms. Table 1 presents the column descriptions, which are referred to as C<sub>1</sub> for the control unmodified monolith, C<sub>2</sub> for the monolith modified with octadecylamine, and C<sub>3</sub> for the monolith modified with benzylamine. Fig. 1 presents a photograph of the stationary phase pushed out of the column after preparation and washing. The resulting stationary phases using this procedure were rigid, coherent, and continuous one-piece separation media.

### 3.2 Stationary phase characterization

The synthesized monolith materials have been characterized by SEM, TGA, FT-IR spectroscopy, and specific surface area analysis. The morphology and the continuous structures of the synthesized monoliths before and after modifications have been explored by using the bulk region SEM micrographs. The bulk region SEM images exposed a significant change in the monolithic morphologies. While the control monolith renders

Table 1 Column descriptions and some of their characterization values

Col.	Description	Porosity <sup>a</sup> (%)	Permeability <sup>b</sup> (m <sup>2</sup> )	Permeability <sup>c</sup> (m <sup>2</sup> )	Specific surface area <sup>d</sup> (m <sup>2</sup> g <sup>-1</sup> )
C <sub>1</sub>	Control monolithic column	81	$1.07 \times 10^{-14}$	$1.35 \times 10^{-14}$	17.27
C <sub>2</sub>	Modification with octadecylamine	75	$6.92 \times 10^{-15}$	$8.76 \times 10^{-15}$	36.01
C <sub>3</sub>	Modification with benzylamine	72	$6.34 \times 10^{-15}$	$8.07 \times 10^{-15}$	38.95

<sup>a</sup> Porosity values measured by injecting a small plug of acetonitrile as unretained material. <sup>b</sup> Permeability values measured by passing acetonitrile through the columns at a flow rate of 0.25 mL min<sup>-1</sup> and 30 °C column temperature. <sup>c</sup> Permeability values measured by passing water through the columns at a flow rate of 0.25 mL min<sup>-1</sup> and 30 °C column temperature. <sup>d</sup> Specific surface area results determined using the adsorption-desorption isotherm of liquid N<sub>2</sub> at -196 °C.

a permeable medium with a uniform and smooth micro-globule structure (Fig. 2A), the surface of the monoliths modified with octadecylamine (Fig. 2B) and with benzylamine (Fig. 2C) became rougher with larger clusters. Although the thermal stability of the stationary phase is an essential prerequisite for GC columns, the TGA results can be used to track the difference between the monoliths before and after modifications. The typical TGA plots demonstrated in Fig. 2D show that the degradation starts at about 170 °C for the unmodified monolith. On the other hand, the modified monoliths with octadecylamine and benzylamine exhibited better thermal stability and did not reveal any remarkable degradation below 260 °C and 275 °C, respectively.

To confirm the expected structures of the monoliths and the post-modification reactions, the polymer monoliths were examined by FT-IR spectroscopy. All spectra exhibit the presence of the peaks at 1165 and 1735  $\text{cm}^{-1}$ , corresponding to the ester of the methacrylate groups C–O and C=O groups, respectively. The disappearance of distinctive anhydride bands at 1779, 1825, and between 1050 and 1040  $\text{cm}^{-1}$  corresponding to the C=O and CO–O–CO stretching bands, indicated the insertion of functional groups into the monolith and successful amidation. IR spectra of the modified monoliths with octadecylamine (Fig. 2E) and benzylamine (Fig. 2F) exhibited stretch bands for O–H hydroxyl and C=O amide at 3415 and 1633  $\text{cm}^{-1}$ , respectively.

The specific surface area of the synthesized monoliths before and after modifications was determined using liquid nitrogen physisorption based on the BET method. The specific surface area of the unmodified control monolith, monolith modified with octadecylamine, and monolith modified with benzylamine was 17.27, 36.01, and 38.95  $\text{m}^2 \text{g}^{-1}$ , respectively. Obviously,

these results confirmed that the amidation reactions induced significant improvement in the specific surface area, which contributes to introducing more interactive sites to improve the retention properties of the monoliths. The specific surface area results are displayed in Table 1.

### 3.3 Column evaluation

The stability of the stationary phase inside the columns and the performance of the separation columns are very important for successful chromatographic processes. The stability of the monoliths inside the columns was examined in terms of the applicable mobile phase flow rate, common liquid chromatography solvents, column pressure and temperature, and operation time.

The commonly used chromatographic solvents acetonitrile and water were used as eluents for the measurement of the column backpressures at flow rates ranging from 0.05 to 0.5  $\text{mL min}^{-1}$ . Fig. 3(A) demonstrates the pressure drop as a measure of column stability *versus* the acetonitrile flow rate. The figure shows a linear relationship between the solvent flow rate and column backpressure at 30 °C for the control and functionalized monolith columns. A linear dependence with regression factors better than 0.9991 indicates that the permeability and mechanical stability of the three columns are excellent.

The stability of the columns has been also assessed against temperature. Fig. 3(B) shows column backpressures *versus* temperature curves of acetonitrile as an eluent at a constant flow rate of 0.25  $\text{mL min}^{-1}$  over a temperature range of 30–70 °C for the control and functionalized monolith columns. As expected, an inversely proportional linear relationship was

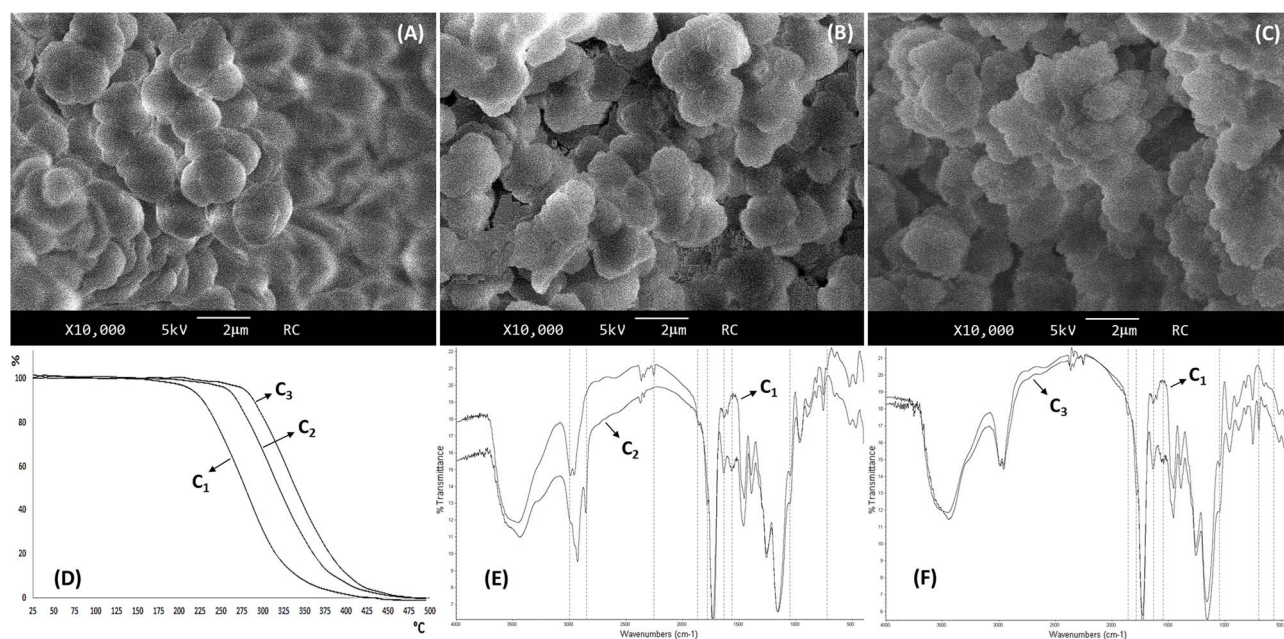


Fig. 2 SEM images of the itaconic anhydride monolith (A), the monolith modified with benzylamine (B), and the monolith modified with octadecylamine (C). TGA curves of the synthesized and modified monoliths (D). FT-IR spectra of the itaconic anhydride monolith and the monolith modified with benzylamine (E) and itaconic anhydride monolith and the monolith modified with octadecylamine (F).

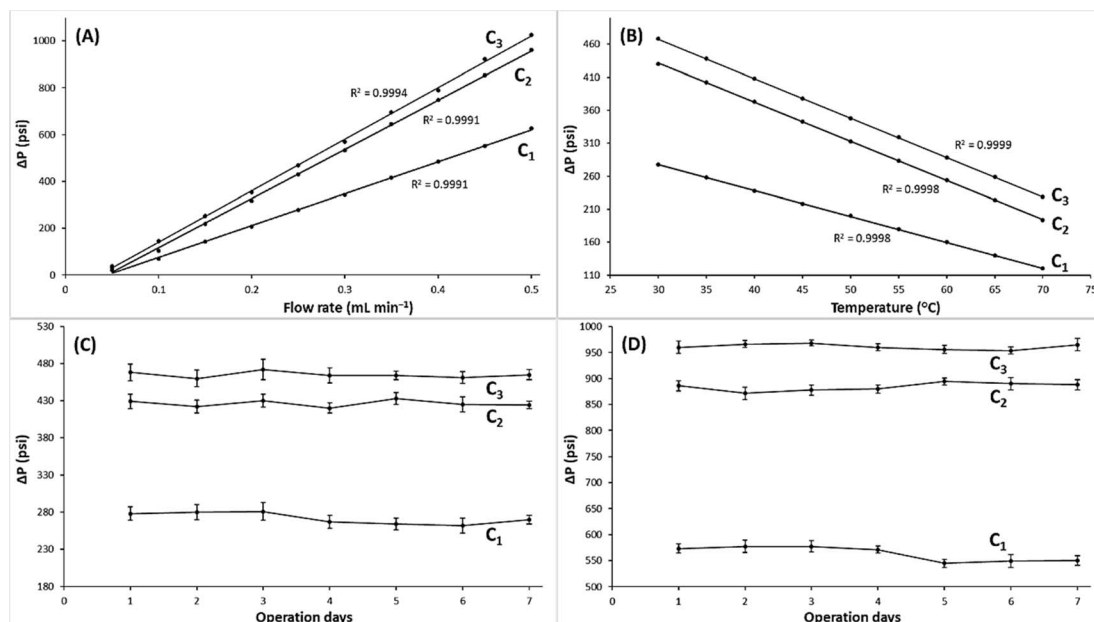


Fig. 3 (A) Column pressures versus flow rate curves of acetonitrile as an eluent at a column temperature of 30 °C for the control and functionalized monolith columns. (B) Column pressures versus temperature curves of acetonitrile as an eluent at a constant flow rate of 0.25 mL min<sup>-1</sup> for the control and functionalized monolith columns. (C) Plots of pressure drop versus operation days as acetonitrile passed through the columns at a 0.25 mL min<sup>-1</sup> flow rate. (D) Plots of pressure drop versus operation days as water passed through the columns at a 0.25 mL min<sup>-1</sup> flow rate.

observed between the column backpressure and temperature which is due to the reduction of the eluent viscosity. The stability of the prepared columns has been investigated over seven consecutive days. As shown in Fig. 3(C and D), the columns exhibit very good backpressure stabilities over the operating times at the same flow rate of 0.25 mL min<sup>-1</sup> using acetonitrile and water as eluents at 30 °C. In conclusion, the linear dependence of the prepared column pressure drops versus eluent flow rate, temperature, and over successive operation days indicates the excellent stability of the monoliths inside the stainless-steel columns and confirms that there is no bleeding of the stationary phases from the columns.

In all cases, the monolith modified with benzylamine for the C<sub>3</sub> column exhibited more backpressure than the monolith modified with octadecylamine for the C<sub>2</sub> column. This difference may be attributed to steric hindrance in the case of the functionalization of the monolith with octadecylamine, and an increased amidation yield in the case of the benzylamine modification. These results are confirmed by using the determined values of the porosity and permeability of the prepared columns. The value of the total porosity of the control column has been reduced by 6% (from 81% to 75%) and by 9% (from 81% to 72%) after the functionalization of the monolith with octadecylamine and benzylamine, respectively.

The permeability of the modified monoliths, on the other hand, has decreased as a result of decreasing the porosity of the columns and increasing the column backpressure values. The numerical permeability values of the prepared columns were determined while acetonitrile and water passed through the columns at a 0.25 mL min<sup>-1</sup> eluent flow rate. The permeability

values of the prepared columns decreased from  $6.92 \times 10^{-15} \text{ m}^2$  for C<sub>2</sub> to  $6.34 \times 10^{-15} \text{ m}^2$  for C<sub>3</sub> using acetonitrile and from  $8.76 \times 10^{-15} \text{ m}^2$  for C<sub>2</sub> to  $8.07 \times 10^{-15}$  for C<sub>3</sub> using water, corresponding to about a  $38 \pm 6$  psi increase in backpressure for the monolith modified with octadecylamine and benzylamine, respectively. The total porosity and permeability values of the prepared columns are summarized in Table 1.

### 3.4 Chromatographic performance

The applicability of the separation columns and the effect of the post-modifications were evaluated for the separation of alkylbenzenes and some polycyclic aromatic hydrocarbons (PAHs). For this purpose, the three columns have been pushed to their optimum chromatographic performance, and the main chromatographic parameters were measured and evaluated.

**3.4.1 HPLC separation of alkylbenzenes.** To explore the effect of monolith amidation on the separation of alkylbenzenes, a comparative study was performed between the control column C<sub>1</sub> and the functionalized columns C<sub>2</sub> and C<sub>3</sub>, to separate a mixture of five alkylbenzenes, toluene, ethylbenzene, *n*-propylbenzene, *n*-butylbenzene, and *n*-pentylbenzene. In all cases, the control column failed to completely separate the analytes under various isocratic and gradient elution conditions. On the other hand, the five alkylbenzenes were totally separated with good resolution values: 1.98–3.86 for column C<sub>2</sub> and 1.77–2.49 for column C<sub>3</sub>. Under the same separation conditions, C<sub>2</sub> exhibits longer run times and the stationary phase reveals more interaction with the analytes as shown in Fig. 4. Obviously, functionalization of monoliths with C<sub>18</sub> groups provides more hydrophobic interactions which

enhances the retention of alkylbenzenes. Practically, the capacity factor for the five alkylbenzenes ranged from 0.78 and 0.65 for toluene to 3.28 and 2.28 for *n*-pentylbenzene using C<sub>2</sub> and C<sub>3</sub> columns, respectively, while the selectivity factors were almost unchanged,  $1.42 \pm 0.05$  for column C<sub>2</sub> and  $1.36 \pm 0.03$  for column C<sub>3</sub>. These results indicate a good balance between run time and the chromatographic resolution of the studied compounds. Fig. 4 presents the typical separation chromatograms of the alkylbenzenes using the control monolith and monolith modified columns under the same separation conditions utilizing acetonitrile/water (60 : 40, v/v) at 0.30 mL min<sup>-1</sup> and a detection wavelength of 254 nm.

The efficiency of the functionalized columns was measured in terms of the height equivalent to a theoretical plate for each analyte at different flow rates ranging from 0.10 to 0.50 mL min<sup>-1</sup>. Fig. S1 (ESI†) illustrates the van Deemter curves for some of the studied compounds. The prepared columns exhibited the best efficiency for *n*-pentylbenzene with 16.24 μm at 0.30 mL min<sup>-1</sup> for column C<sub>2</sub>, while the highest performance value using column C<sub>3</sub> was observed for *n*-propylbenzene with 18.34 μm at 0.25 mL min<sup>-1</sup> flow rate. Regarding the shape of the peaks, low tailing factors were observed with asymmetry measured at 10% of the peak heights of  $A_s \leq 1.12$  in all cases. The chromatographic parameters of alkylbenzene separation were calculated under optimized conditions and are provided in Table 2.

**3.4.2 HPLC separation of PAHs.** The prepared columns were also tested for the separation of some PAHs such as naphthalene, acenaphthylene, fluorine, phenanthrene, anthracene, pyrene, benzo(*a*)anthracene, chrysene, and benzo(*k*)fluoranthene. Again, under all isocratic and gradient conditions, the control column was unable to separate the analytes. The

nine PAHs, on the other hand, were fully separated after the functionalization of the monolith with good resolution values;  $\geq 1.12$  for column C<sub>2</sub> and  $\geq 2.38$  for column C<sub>3</sub>. For the purpose of comparing columns, PAHs have been separated under the same chromatographic conditions using columns C<sub>2</sub> and C<sub>3</sub>. Fig. 5 shows the typical chromatograms for the PAHs separated under the same gradient elution conditions as follows: 0 → 15 min (30% acetonitrile), 15 → 40 min (linear gradient 30% → 90% acetonitrile), and 40 → 60 min (90% acetonitrile). The flow rate was fixed at 0.10 mL min<sup>-1</sup> and the detector wavelength was set at 230 nm. The enhancement in the analyte's retention performance using the modified monoliths is suggested to be due to the smaller pores introduced by the functionalization process and the higher surface area of the modified over the control monolith. However, the presence of benzyl groups within the monolith structure of column C<sub>3</sub> also improved the separation and retention of the PAHs through the strong  $\pi$ - $\pi$  interactions.

Under the mentioned chromatographic conditions, the capacity factors gradually increased, whereas the change in selectivity factors for all analytes was limited at values of 1.07–1.20 for column C<sub>2</sub> and 1.11–1.28 for column C<sub>3</sub>. These features prove the suitability of stationary phases for complete separation and accurate quantitation of PAHs. While the flow rate increased from 0.10 to 0.50 mL min<sup>-1</sup>, the efficiency of the prepared columns was measured for each compound and van Deemter plots were obtained as displayed for some of the studied compounds shown in Fig. S1 (ESI†). The highest performance in terms of the height equivalent to a theoretical plate was observed for chrysene with 9.58 μm for column C<sub>2</sub> at 0.30 mL min<sup>-1</sup>, and 4.08 μm exhibited for column C<sub>3</sub> at 0.25 mL min<sup>-1</sup>. Low peak tailings were observed for all PAHs, with

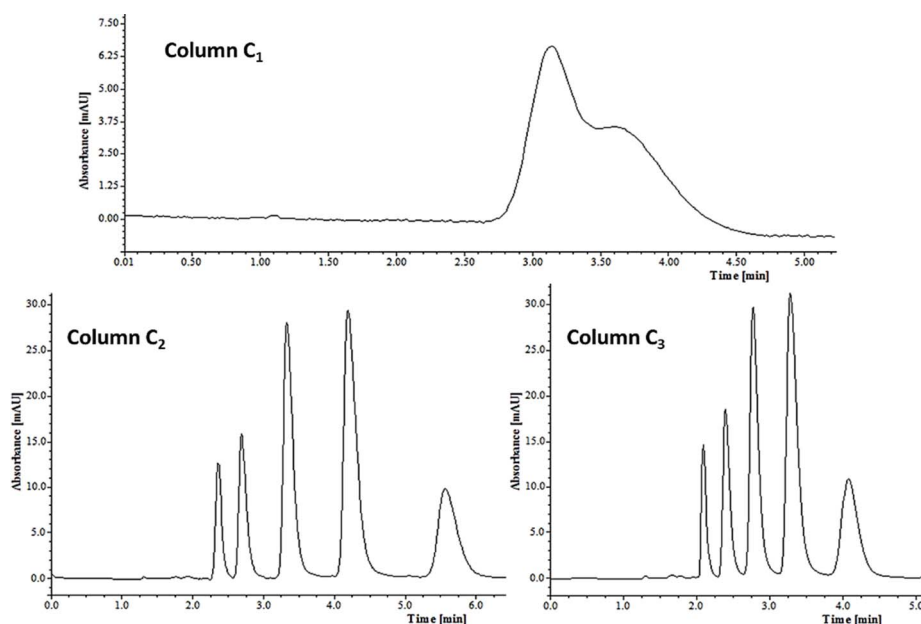


Fig. 4 Typical chromatograms of the alkylbenzene separation using the control column (up), the column modified with benzylamine (down left), and the column modified with octadecylamine (down right) under the optimal conditions of each column using acetonitrile/water as the isocratic elution mobile phase. Peaks by order of elution: toluene, ethylbenzene, *n*-propylbenzene, *n*-butylbenzene, and *n*-pentylbenzene.

**Table 2** Peak and column efficiency parameters for the separation of the studied mixtures using the C<sub>2</sub> and C<sub>3</sub> columns expressed in terms of  $t_R$ ,  $H$ ,  $k$ ,  $\alpha$ ,  $R_s$ , and  $A_s$  under the optimal conditions<sup>a</sup>

Solute	C <sub>2</sub> column						C <sub>3</sub> column						
	$t_R$	$H$	$k$	$\alpha$	$R_s$	$A_s$	$t_R$	$H$	$k$	$\alpha$	$R_s$	$A_s$	
Alkylbenzenes	Toluene	2.36	20.30	0.78	—	—	1.08	2.07	21.07	0.65	—	—	1.11
	Ethylbenzene	2.72	19.38	1.09	1.38	1.98	1.05	2.44	21.82	0.92	1.39	1.77	1.07
	<i>n</i> -Propylbenzene	3.34	18.04	1.52	1.39	2.44	1.06	2.78	19.02	1.23	1.33	1.85	1.10
	<i>n</i> -Butylbenzene	4.23	18.86	2.20	1.44	3.08	1.11	3.29	20.71	1.65	1.34	2.16	1.08
	<i>n</i> -Pentylbenzene	5.54	16.24	3.28	1.48	3.86	1.12	4.11	25.02	2.28	1.38	2.49	1.05
PAHs	Naphthalene	10.43	39.49	7.27	—	—	1.13	11.53	31.50	7.78	—	—	1.07
	Acenaphthylene	12.35	26.56	8.80	1.20	1.66	1.15	14.99	18.07	10.42	1.28	3.02	1.13
	Fluorine	13.77	28.30	9.91	1.12	1.15	1.18	18.07	12.43	12.77	1.22	2.71	1.14
	Phenanthrene	14.97	18.03	10.89	1.09	1.12	1.09	20.82	9.93	14.87	1.16	2.38	1.14
	Anthracene	17.83	14.31	13.15	1.20	2.42	1.07	25.46	8.48	18.41	1.23	3.72	1.08
	Pyrene	20.47	18.62	15.24	1.15	1.89	1.19	30.35	9.61	22.15	1.20	3.26	1.21
	Benzo( <i>a</i> )anthracene	23.74	11.03	17.84	1.17	2.19	1.06	37.50	4.42	27.61	1.24	4.63	1.05
	Chrysene	25.46	9.59	19.20	1.07	1.24	1.08	40.93	4.08	30.22	1.11	2.38	1.05
Benzo( <i>k</i> )fluoranthene	30.25	33.39	23.01	1.19	2.11	1.05	48.57	13.82	36.06	1.19	3.25	1.09	

<sup>a</sup>  $t_R$ : retention time (min),  $H$ : height equivalent to theoretical plates ( $\mu\text{m}$ ),  $k$ : capacity factor,  $\alpha$ : selectivity factor,  $R_s$ : resolution factor, and  $A_s$ : peak asymmetry measured at 10% of peak heights.

asymmetry factors measured at 10% of the peak heights of  $\leq 1.21$  in all cases. The whole determined parameters of PAH compound separation are presented in Table 2.

### 3.5 Repeatability and reproducibility study

To assess the repeatability of the injections on the same column and the reproducibility of the prepared columns, three parameters including retention time, the height equivalent to a theoretical plate, and resolution have been selected and estimated in terms of percent relative standard deviation (%RSD) for some of the studied compounds.

For the reproducibility tests, six extra columns; three each of C<sub>2</sub> and C<sub>3</sub>, have been prepared and modified with the same procedure and used for the separation of alkylbenzenes under the same conditions. In all cases and for both columns, the repeatability levels were  $\leq 9.42\%$  ( $n = 5$ ) based on run-to-run injections and  $\leq 9.48\%$  ( $n = 5$ ) based on day-to-day injections for 5 successive days. These values confirmed that the prepared columns have good precision in terms of intraday and interday injections of the solutes. On the other hand, injection of alkylbenzenes into the other prepared columns shows lower reproducibility. For the two types of columns, the determined

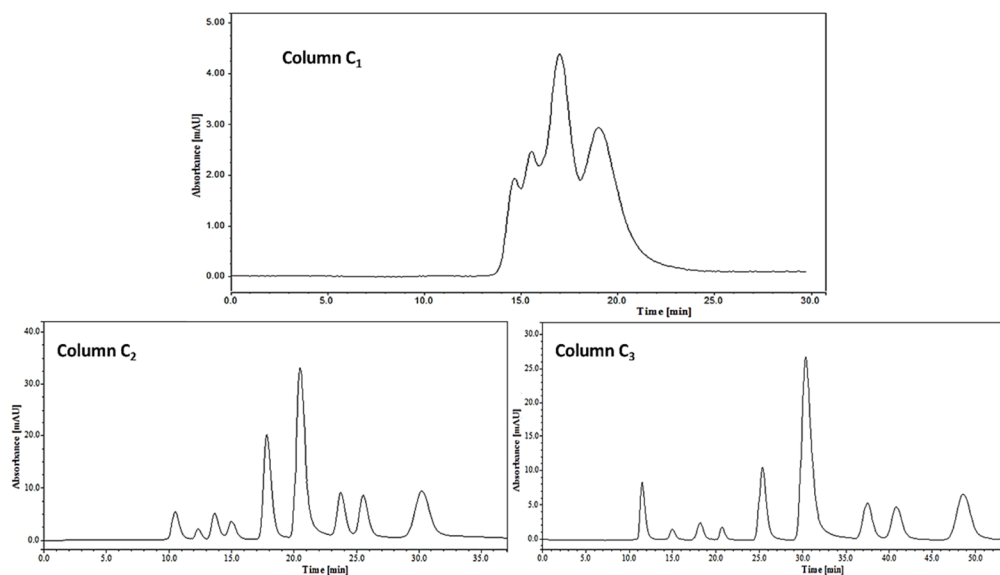


**Fig. 5** Typical chromatograms of the PAH separation using the control column (up), the column modified with benzylamine (down left), and the column modified with octadecylamine (down right) under the optimal conditions of each column using acetonitrile/water as the gradient elution mobile phase. Peaks by order of elution: naphthalene, acenaphthylene, fluorene, phenanthrene, anthracene, pyrene, benzo(*a*)anthracene, chrysene, and benzo(*k*)fluoranthene.

values of %RSD were  $\leq 11.14\%$  ( $n = 4$ ) for retention time,  $\leq 20.95\%$  ( $n = 4$ ) for height equivalent of the theoretical plate, and  $\leq 8.23$  ( $n = 4$ ) for the resolution between the peaks. The results revealed very good repeatability values for the mixtures injected in the columns and lower reproducibility values on different columns. This could be explained by the presence of several preparation steps including polymerization of the monolith material and post-polymerization modification of the monoliths, in addition to the other chromatographic variables. The complete repeatability and reproducibility results are presented in Table S1 (ESI<sup>†</sup>).

### 3.6 Analysis of real samples

The validity of the prepared monolithic columns was tested for the separation of the active ingredients extracted from some commercial pharmaceutical formulations including Profinal-XP tablets, Relaxon capsules, and Aspirin-C tablets consisting of caffeine and ibuprofen, paracetamol and chlorzoxazone, and aspirin and vitamin-C, respectively. Fig. S2–S4 (ESI<sup>†</sup>) show the separation chromatograms for the extracted solutions under optimum chromatographic conditions for each drug. Under the optimal separation conditions, complete baseline separations were accomplished for the active compounds of the three pharmaceutical preparations with  $R_s \geq 2.02$ ,  $H \leq 38.6 \mu\text{m}$ , and  $A_s \leq 1.33$  in all cases.

The reliability of the prepared monolithic columns was also examined for the separation of black tea water extract constituents. Fig. S5 (ESI<sup>†</sup>) displays the successful separation chromatogram of some contents of the tea water extract. The optimized method illustrates that the  $R_s$  values of the three detected compounds (gallic acid, theobromine, and caffeine) were 2.83 and 4.16. These values revealed a good compromise between  $R_s$  and the runtime (12 min). The efficiency of the separation column in terms of  $H$  values was  $\leq 60.2 \mu\text{m}$  at the optimum flow rates. All validation parameters proved the suitability of the prepared columns and the optimized methods for quality control and routine analysis of the drugs in their combined pharmaceutical preparations and methylxanthines in tea samples.

### 3.7 Comparison with other studies

In this part, the prepared columns have been compared with those in other reported studies for the separation of PAHs. The comparison parameters of the prepared columns with other reported methods (published in 2014 and beyond) for the separation of PAH compounds are summarized in Table S2 (ESI<sup>†</sup>). To the best of our knowledge, previous research mostly used analytical scales of HPLC column dimensions packed with commercial  $C_{18}$  particulate silica-based stationary phases. In terms of the performance of the separation columns, it's difficult to make an honest comparison since most of the previous studies aimed to develop extraction methods for estimating PAHs in different samples. Unfortunately, few researchers estimate chromatographic parameters and evaluate the performance of the separation columns towards PAHs. However, the prepared columns showed some

advantages over other prepared columns in terms of the theoretical plates, capacity factors, tailing factors, and the number of separated compounds.

In comparison with the conventional scale columns (4.6 mm i.d.) typically operated at 0.5–1.5 mL min<sup>-1</sup> flow rate, the prepared columns showed advantages in terms of lower solvent and sample consumption. This is obvious in the eluent consumption which is notably lower at this scale (6.0 mL h<sup>-1</sup>) than with conventional scale columns (30–90 mL h<sup>-1</sup>). On the other hand, the amount and cost of a homemade polymer monolith material are significantly lower than that of the particulate silica-based  $C_{18}$  stationary phases and require less preparation effort, starting materials, and simpler preparation steps, and hence, less cost and chemical generation relative to conventional scale columns. Based on their chromatographic performance, cost-effectiveness, and minimal waste generation, in addition to their easy functionalization, diversity, and tunability, the prepared poly(itaconic anhydride-co-ethylene dimethacrylate) monoliths and the proposed post-polymerization modification have been shown to be very useful and acceptable alternatives to the commercial  $C_{18}$  packed columns for the routine determination of PAH chemicals.

## 4. Conclusions

In the present work, polymer monoliths are prepared *via* cyclic anhydride ring-opening polymerization as tunable platform stationary phases for chromatographic applications. Then, the reactive anhydride was successfully functionalized using two primary amine compounds (octadecylamine and benzylamine). The ultimate aim of this research is to improve the separation efficiency of polymer-based monoliths. Practically, the functionalization of monoliths with octadecylamine provided more hydrophobic interactions and enhanced the retention of alkylbenzenes, while the modification of monoliths with benzyl groups improved the separation and increased retention of the PAHs through the strong  $\pi$ - $\pi$  interactions. However, based on the monolith characterization results, the post-modification polymerization not only enhances the separation efficiency of the prepared columns toward mixtures of alkylbenzenes and PAHs, but also promotes and diversifies their chemical properties and functionality, increases their surface area, and improves their thermal and mechanical stability.

This work provides more approaches by representing functionalities within other reactive monomers such as amino acids *N*-carboxy anhydride, maleic anhydride, vinyl azlactone, glycidyl methacrylate, and *N*-hydroxy succinimide. These reactive platforms are potentially suitable for further modifications with alcohols through esterification or amines through amidation, according to the desired interaction and chemical separation. Important candidates in this regard may include some amino acids, carbohydrates, antibodies, and proteins. All the evaluation studies and the chromatographic results provide evidence to demonstrate that the prepared columns could be applied to test real samples, especially in environmental applications.



## Author contributions

Ahmad Aqel: conceptualization, investigation, formal analysis, funding acquisition, and writing original draft. Ayman A. Ghfar: project administration, data curation, software, and validation. Ahmed-Yacine Badjah-Hadj-Ahmed: visualization, methodology, and review and editing. Zeid A. ALOthman: resources, supervision, verifying information, and review and editing.

## Conflicts of interest

There are no conflicts to declare.

## Acknowledgements

The authors extend their appreciation to the Deputyship for Research & Innovation, “Ministry of Education” in Saudi Arabia for funding this research work through the project number (IFKSUDR\_P117).

## References

- 1 F. Svec and Y. Lv, *Anal. Chem.*, 2015, **87**, 250–274.
- 2 K. Lynch, J. Ren, M. Beckner, C. He and S. Liu, *Anal. Chim. Acta*, 2019, **1046**, 48–68.
- 3 S. Ma, Y. Li, C. Ma, Y. Wang, J. Ou and M. Ye, *Adv. Mater.*, 2019, 1902023.
- 4 A. Aqel, Z. A. ALOthman, K. Yusuf, A. Y. Badjah-Hadj-Ahmed and A. A. Alwarthan, *J. Chromatogr. Sci.*, 2014, **52**, 201–210.
- 5 T. Hong, X. Yang, Y. Xu and Y. Ji, *Anal. Chim. Acta*, 2016, **931**, 1–24.
- 6 F. Svec and J. M. J. Frechet, *Anal. Chem.*, 1992, **64**, 820–822.
- 7 M. Nechvátalová and J. Urban, *Anal. Sci. Adv.*, 2022, **3**, 154–164.
- 8 J. Wang, X. Jiang, H. Zhang, S. Liu, L. Bai and H. Liu, *Anal. Methods*, 2015, **7**, 7879–7888.
- 9 M. Gama, F. Rocha and C. Bottoli, *Trends Anal. Chem.*, 2019, **115**, 39–51.
- 10 F. Maya and F. Svec, *Polymer*, 2014, **55**, 340–346.
- 11 S. Lubbad, *J. Chromatogr. A*, 2016, **1443**, 126–135.
- 12 X. Wang, X. Li, X. Jiang, P. Dong, H. Liu, L. Bai and H. Yan, *Talanta*, 2017, **165**, 339–345.
- 13 I. Nischang, I. Teasdale and O. Brüggemann, *Anal. Bioanal. Chem.*, 2011, **400**, 2289–2304.
- 14 S. H. Lubbad and M. R. Buchmeiser, *J. Chromatogr. A*, 2010, **1217**, 3223–3230.
- 15 H. Zhang, J. Ou, Y. Wei, H. Wang, Z. Liu, L. Chen and H. Zou, *Anal. Chim. Acta*, 2015, **883**, 90–98.
- 16 Y. Li, H. D. Tolley and M. L. Lee, *J. Chromatogr. A*, 2011, **1218**, 1399–1408.
- 17 J. Urban, F. Svec and J. M. J. Frechet, *J. Chromatogr. A*, 2010, **1217**, 8212–8221.
- 18 Y. Lv, Z. Lin and F. Svec, *Anal. Chem.*, 2012, **84**, 8457–8460.
- 19 S. Alharthi and Z. El Rassi, *Molecules*, 2020, **25**, 1323.
- 20 H. Wang, J. Ou, H. Lin, Z. Liu, G. Huang, J. Dong and H. Zou, *J. Chromatogr. A*, 2014, **1367**, 131–140.
- 21 K. A. McEwan, S. Slavin, E. Tunnah and D. M. Haddleton, *Polym. Chem.*, 2013, **4**, 2608–2614.
- 22 N. Albekairi, A. Aqel and Z. A. ALOthman, *Chromatographia*, 2019, **82**, 1003–1015.
- 23 M. E. Ibrahim and C. A. Lucy, *Talanta*, 2012, **100**, 313–319.
- 24 P. Zakaria, J. P. Hutchinson, N. Avdalovic, Y. Liu and P. R. Haddad, *Anal. Chem.*, 2005, **77**, 417–423.
- 25 B. Fresco-Cala, E. J. Carrasco-Correa, S. Cárdenas and J. M. Herrero-Martínez, *Microchem. J.*, 2018, **139**, 222–229.
- 26 A. Aqel, S. S. Alzahrani, A. Al-Rifai, M. Alturkey, K. Yusuf, Z. A. ALOthman and A. Y. Badjah-Hadj-Ahmed, *Curr. Anal. Chem.*, 2020, **16**, 223–233.
- 27 S. D. Chambers, F. Svec and J. M. J. Fréchet, *J. Chromatogr. A*, 2011, **1218**, 2546–2552.
- 28 S. D. Chambers, T. W. Holcombe, F. Svec and J. M. J. Fréchet, *Anal. Chem.*, 2011, **83**, 9478–9484.
- 29 A. Aqel, A. A. Ghfar, K. Yusuf, K. M. Alotaibi, R. M. Alafra’a, M. A. Habila, A. Y. Badjah-Hadj-Ahmed and Z. ALOthman, *J. Chromatogr. A*, 2023, **1690**, 463695.
- 30 A. Aqel, M. Obbed, A. A. Ghfar, K. Yusuf, A. M. Alsubhi and A. Badjah-Hadj-Ahmed, *Separations*, 2022, **9**, 389.
- 31 Y. Lv, F. M. Alejandro, J. M. Frechet and F. Svec, *J. Chromatogr. A*, 2012, **1261**, 121–128.
- 32 M. Navarro-Pascual-Ahuir, M. J. Lerma-García, M. J. Ler-Ramos, E. F. Simm-Alfonso and J. M. Herrero-Martínez, *Electrophoresis*, 2013, **34**, 925–934.
- 33 O. Sedlacek, J. Kucka, F. Svec and M. Hruby, *J. Sep. Sci.*, 2014, **37**, 798–802.
- 34 N. Ganewatta and Z. El Rassi, *J. Anal. Sci. Technol.*, 2020, **11**, 39.
- 35 Y. Liu, Y. Chen, H. Yang, L. Nie and S. Yao, *J. Chromatogr. A*, 2013, **1283**, 132–139.
- 36 K. Yusuf, O. Shekhah, A. Aqel, S. Alharbi, A. S. Alghamdi, R. M. Aljohani, Z. A. ALOthman and M. Eddaoudi, *Microporous Mesoporous Mater.*, 2023, **357**, 112630.
- 37 S. Yang, F. Ye, C. Zhang, S. Shen and S. Zhao, *Analyst*, 2015, **140**, 2755–2761.
- 38 X. J. Peng and S. B. Wu, *Chin. J. Anal. Chem.*, 2023, **51**, 100199.
- 39 T. Otsu and J. Z. Yang, *Polym. Int.*, 1991, **25**, 245–251.
- 40 B. Milovanović, C. S. Trifunovic, L. Katsikas and G. Popovic, *J. Serbian Chem. Soc.*, 2007, **72**, 1507–1514.
- 41 K. Y. H. Mahmoud, Z. A. ALOthman and A. S. A. El-Faham, *US Pat.* 9624335B1, 2017.
- 42 J. A. Wallach and S. J. Huang, *Biomacromolecules*, 2000, **1**, 174–179.